



EO for Africa Symposium 2024

23 - 26 September 2024

ESA | ESRIN, Frascati (IT)



EO Africa Water Resource Management: support to farmers and planners to improve irrigation water management

24/09/2024



ESA UNCLASSIFIED - For ESA Official Use Only

1

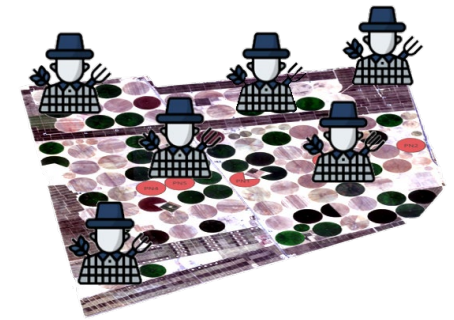




**National Authority for Remote Sensing & Space Sciences (NARSS)
Egypt**



**Investors at October Sixth
for Agricultural Projects - Egypt**



Objectives:

- To map the actual evapotranspiration (ET_a) and thus the actual water consumption of the cultivated crops
- To estimate the irrigation efficiency at regional scale
- To evaluate the impact of introducing low water consumption rice varieties or innovative irrigation practices

Outcomes:

- Creation of a web platform for the integration of ET_a, NDVI and CWSI maps
- An open source ET_a model in Python for estimating the ET_a during summer and winter seasons
- Compare with actual field measurements for evaluation of the approach

SARE model

ET_o varies depending on land cover, elevation, location, weather condition, and Julian day

$$ET_o = V_f * L_f * E_f * S_f * T_f$$

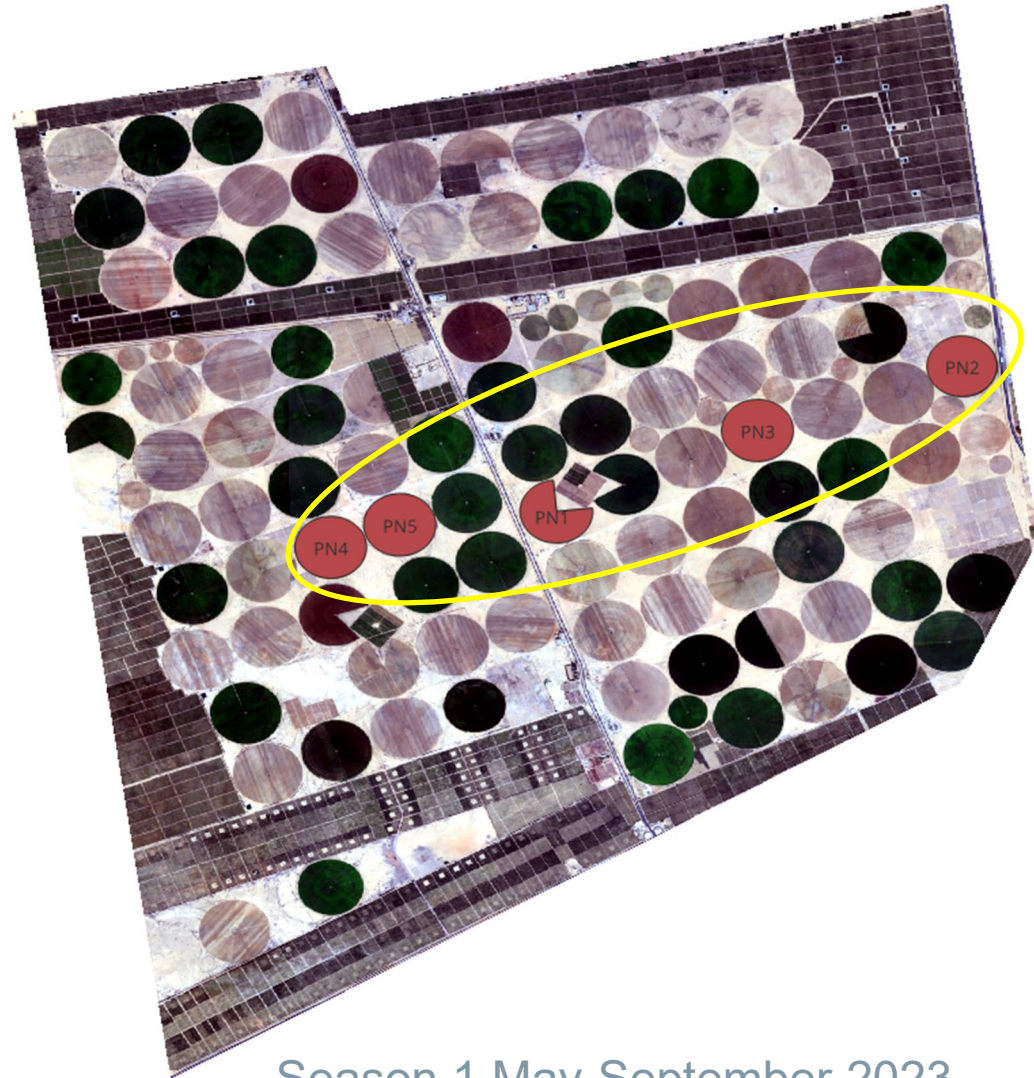
Leading to ET_a = ET_o * K_c * K_s

The SARE algorithm has been applied for each of the EO data combination:

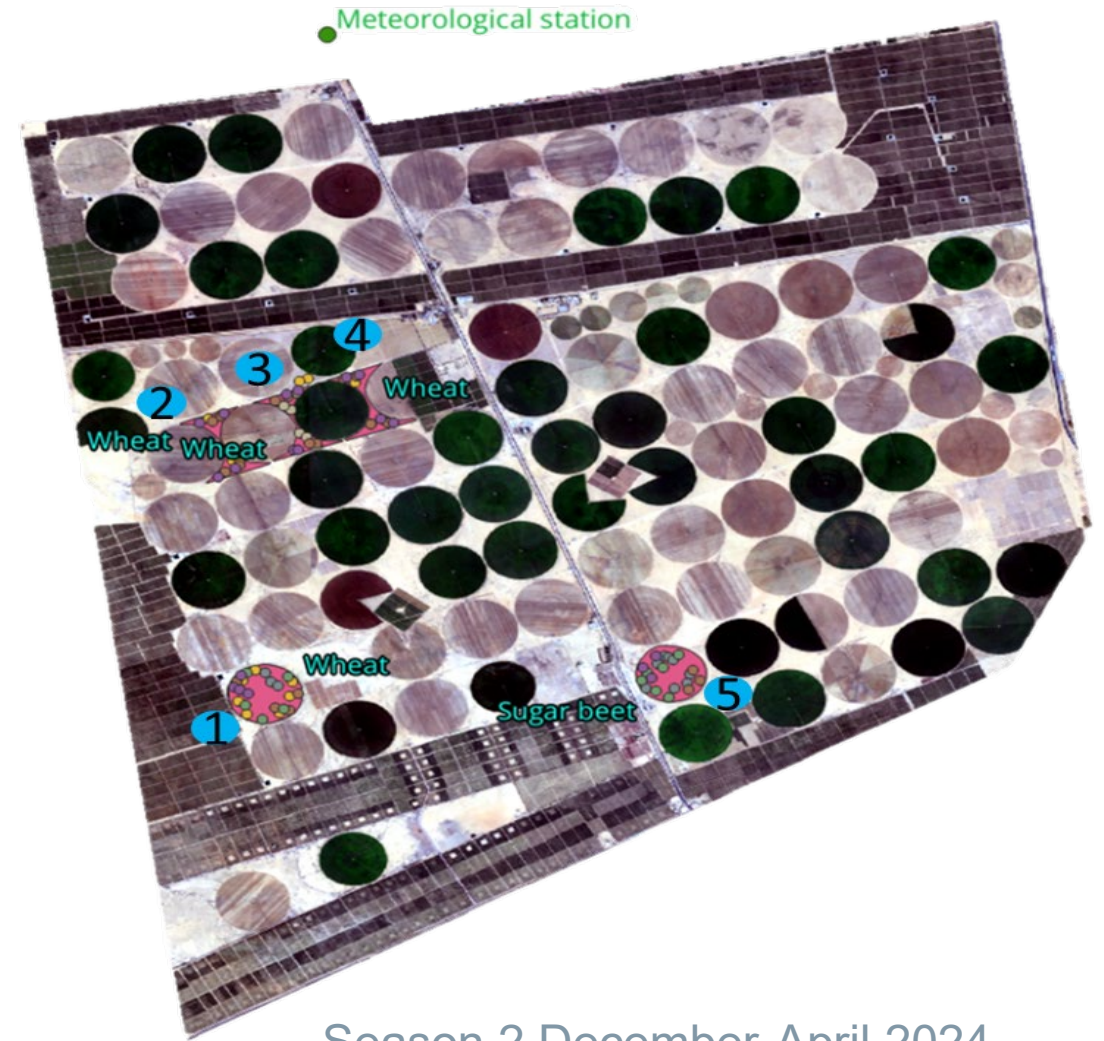
1. Using Sentinel-2 as input for VNIR data and Landsat for TIR data
2. Using Landsat for both VNIR and TIR
3. Using PRISMA as input for VNIR data (using different band configurations) and Landsat for TIR data.

The first two cases have been selected to establish a reference baseline using multispectral sensors to be compared with the results obtained from the hyperspectral sensor .

Region of interest



Season 1 May-September 2023



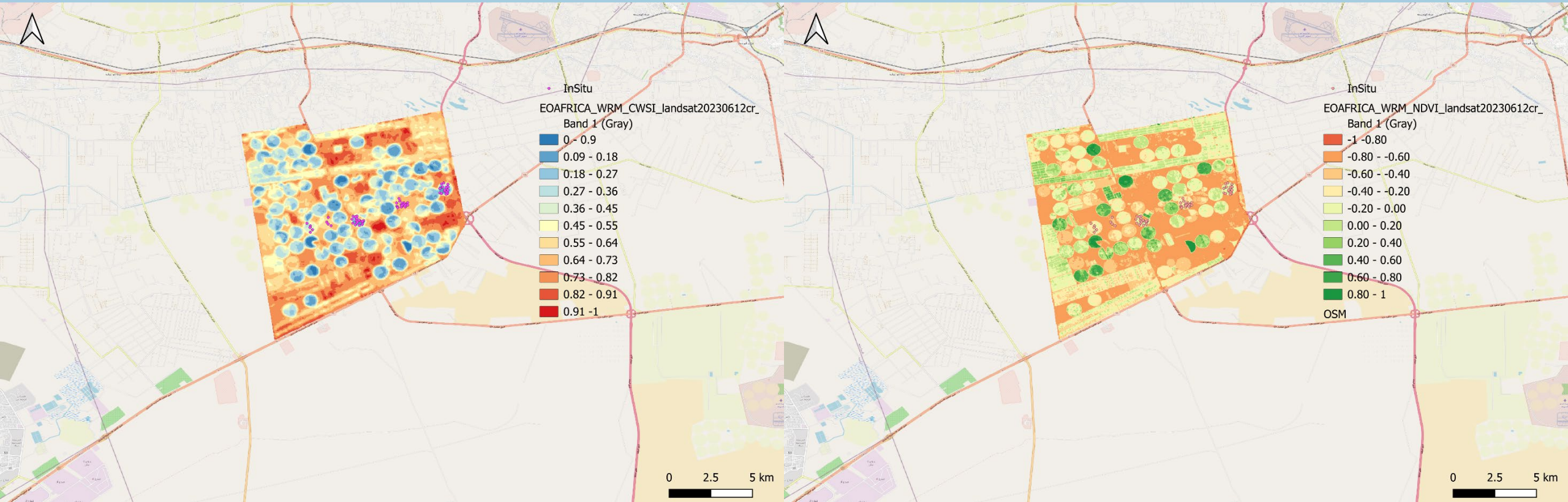
Season 2 December-April 2024

Output Product maps (1/2)



CWSI map

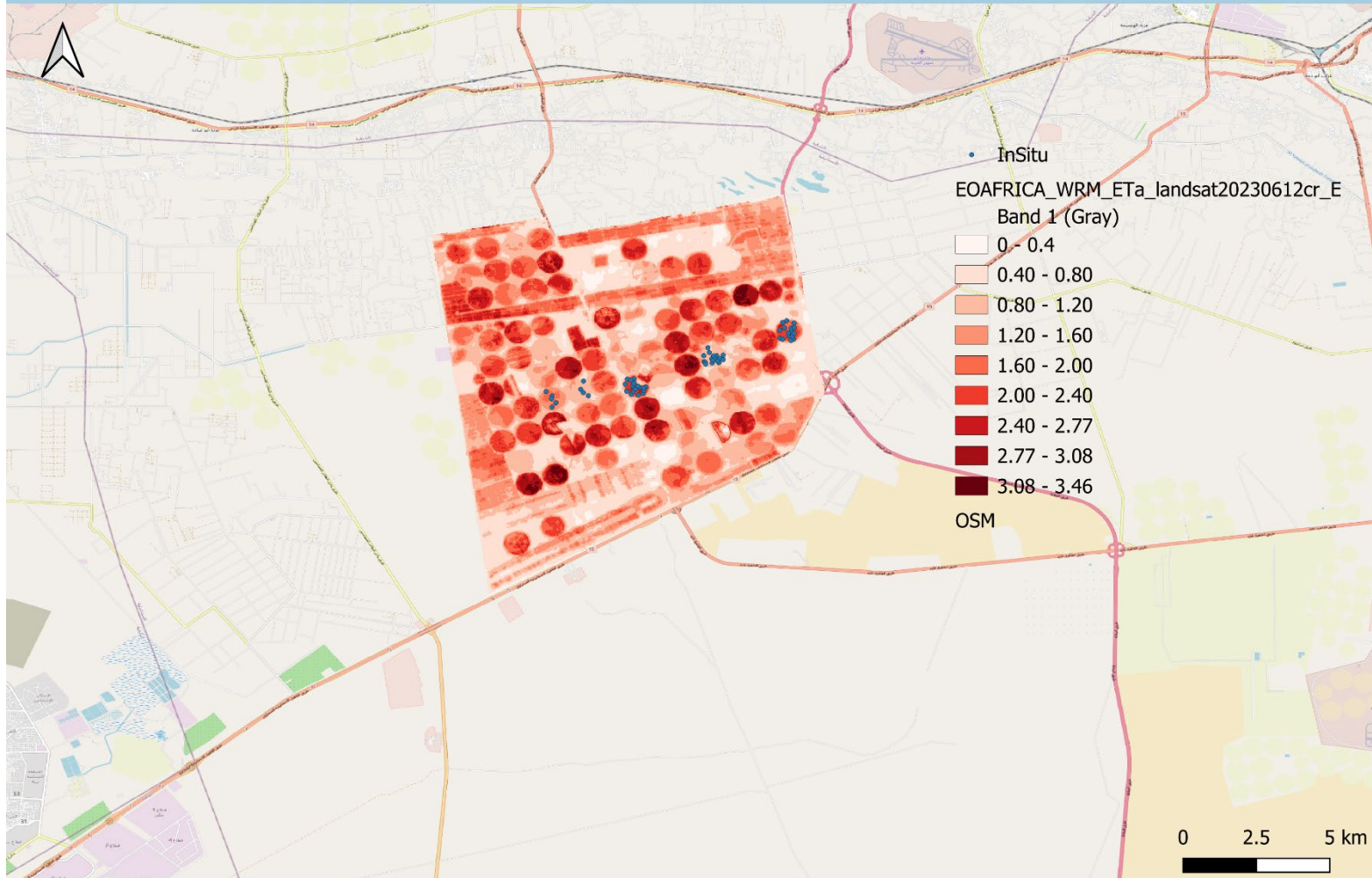
NDVI map



Output Product maps (2/2)



ETa map



Hyperspectral satellite capabilities(PRISMA)



| PRISMA (band # & range) | Sentinel-2 (band # & range) | Landsat (band # & range) |
|---|--|---|
| Red: 32–35 (647–685 nm) NIR: 11–22 (778–905 nm) | Red: #4 (650–680 nm) NIR: #8 (785–899 nm) | Red: #4 (638–673 nm) NIR: #5 (772–898 nm) |
| PRISMA bands selected for “RED” (central wavelength in nm) | | PRISMA bands selected for “NIR” (central wavelength in nm) |
| 655.4 | 785.7 | |
| 664.9 | 796.1 | |
| 674.5 | 806.7 | |
| | 817.3 | |
| | 827.9 | |
| | 838.5 | |
| | 849.2 | |
| | 860.0 | |
| | 870.7 | |
| | 881.5 | |
| | 892.1 | |

Approach 1: Combination of multiple bands

We selected multiple bands in the Red and NIR part of the PRISMA spectrum to match the Red and NIR bands of Sentinel-2 (i.e., Red: 650–680nm; NIR: 785–899nm) and Landsat (i.e., Red: 638–673nm; NIR: 772–898nm)

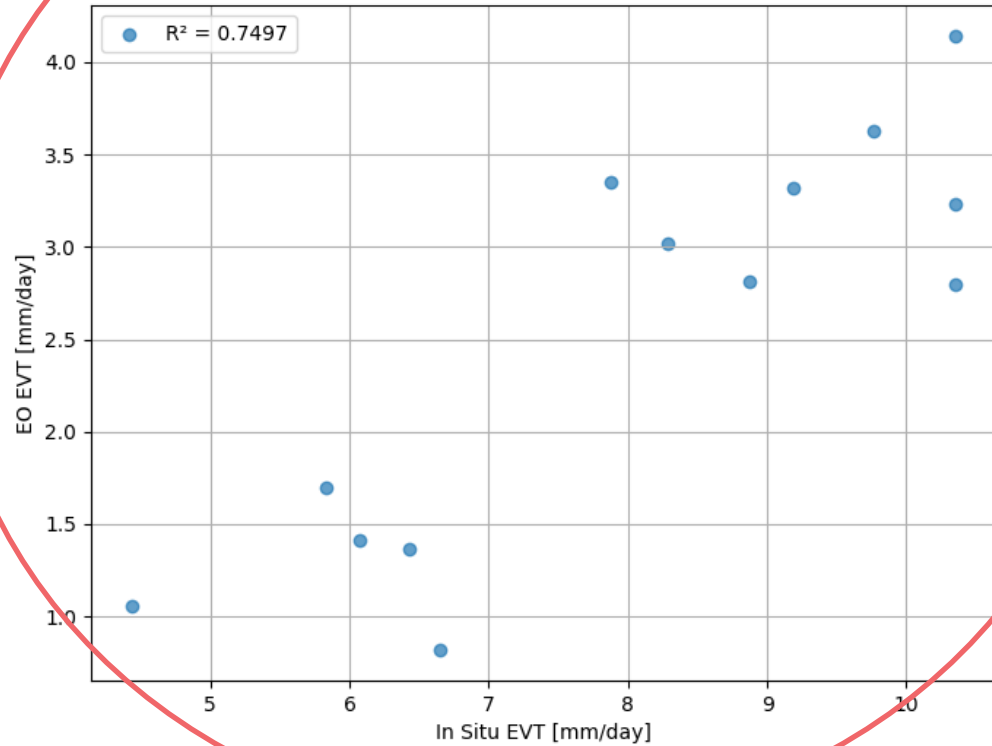
Approach 2: Central wavelength band

We selected a single PRISMA band centered at 664.9 nm (for Red) and at 806.7 nm (for NIR)

21/07/23 Prisma's band combination selections

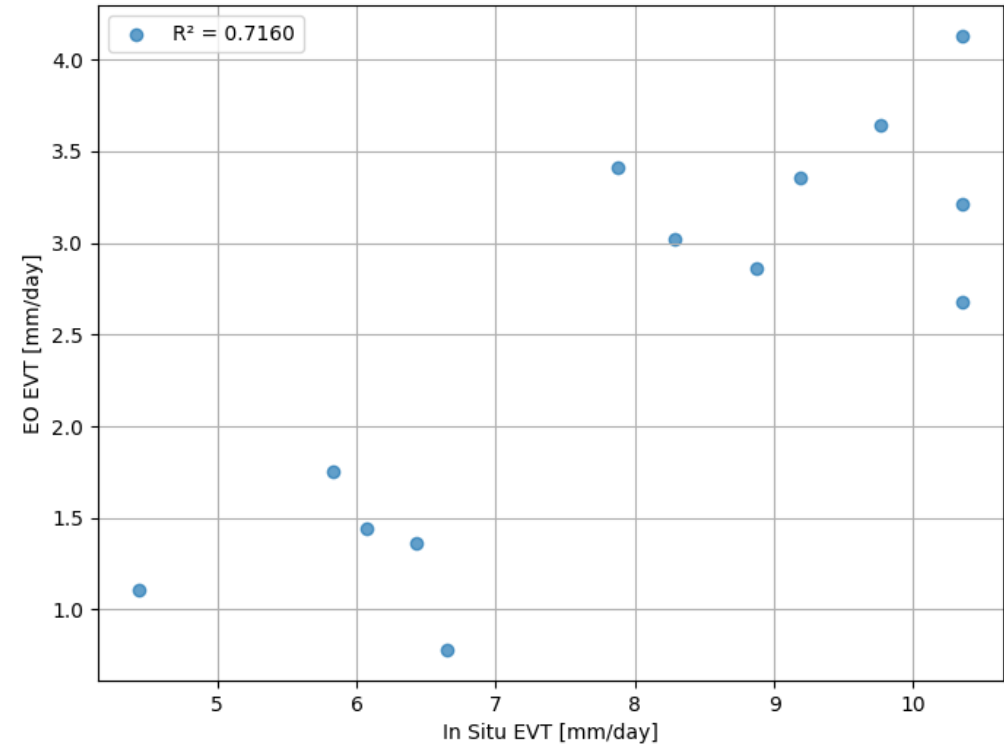
Red at 664.9 nm, NIR at 806.7 nm

EO EVT (using Ks from in situ) vs In Situ EVT



Red at 655.4 nm, NIR 785.7 nm

EO EVT (using Ks from in situ) vs In Situ EVT

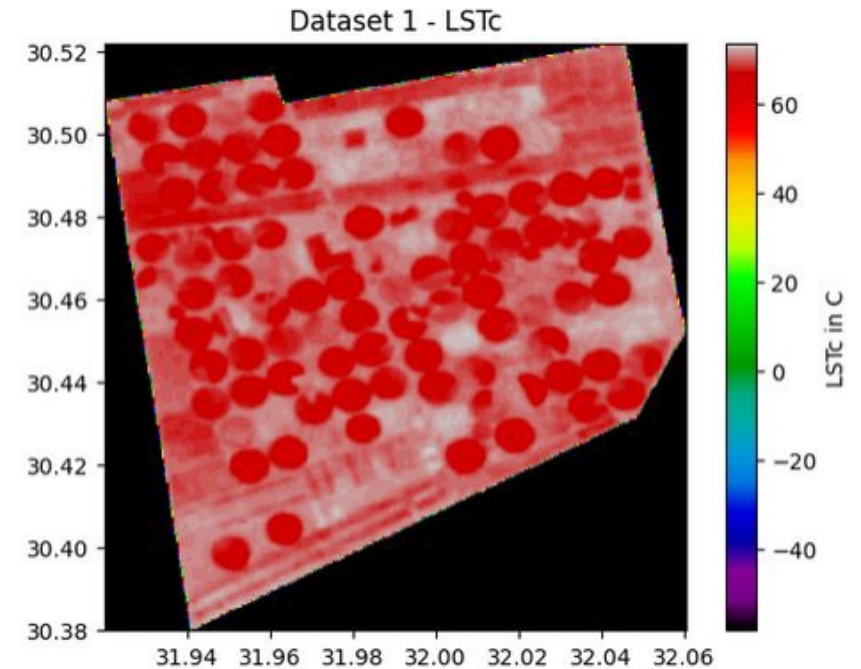
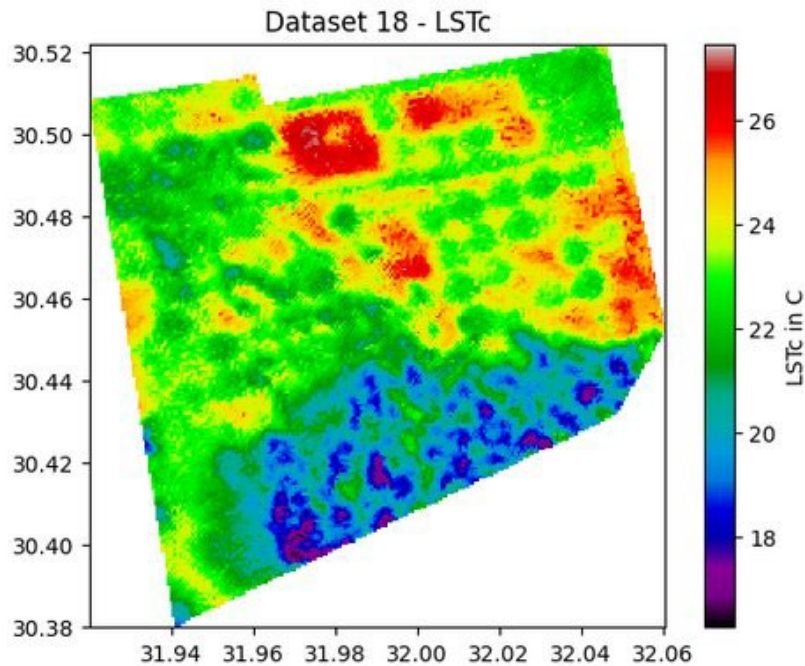


The ECOSTRESS challenge



- ECOSTRESS data are not usable because the acquisitions over the Area of Interest (AOI) occurred at night during the days of in-situ measurements. Using thermal measurements taken at night introduces too much uncertainty into the estimation of K_s .
- ECOSTRESS sensor is not operational – Giving historical data without the option to choose ascending/descending orbit's data, cloud coverage etc.
 - 16/06 Ecostress (night time) LST

16/06 Landsat LST





The stress coefficient K_s value can be estimated using a linear relationship with the air-surface temperature difference as the main parameter.

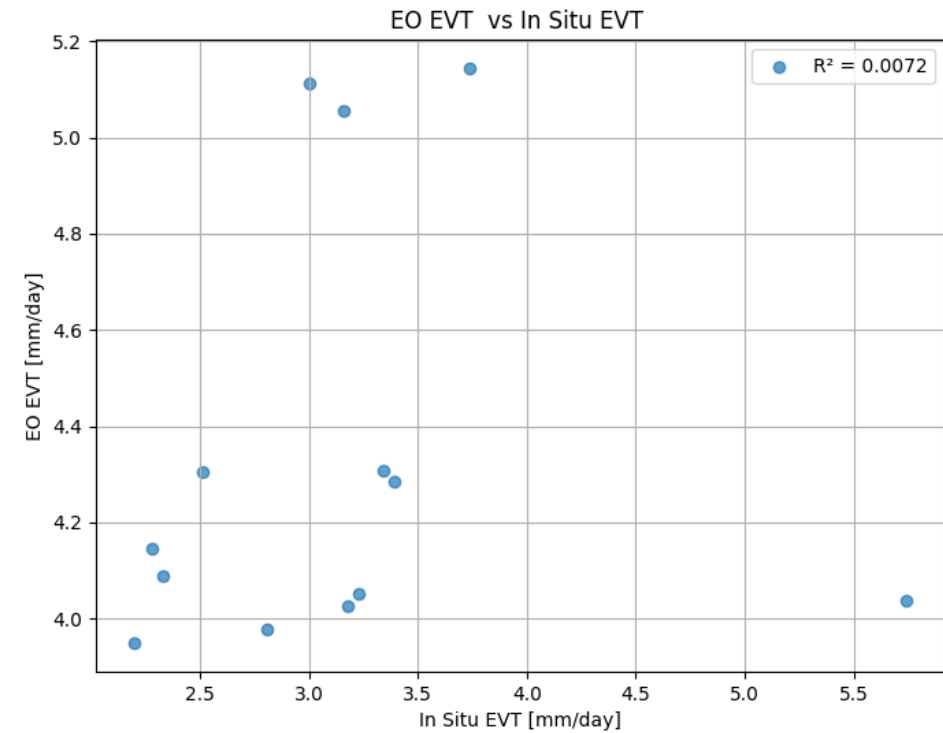
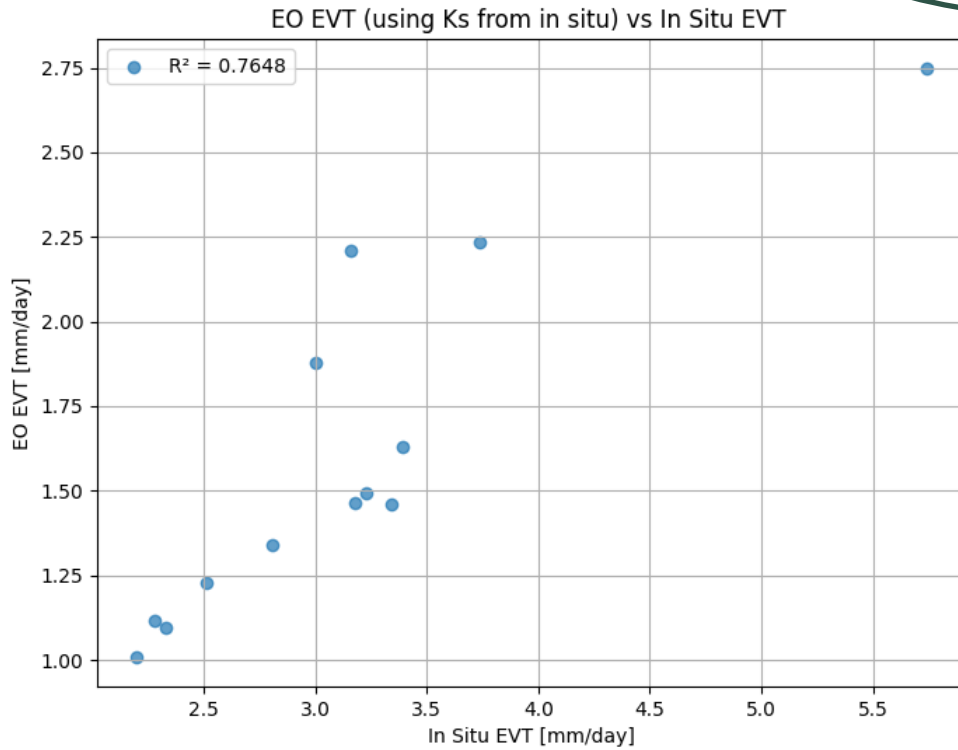
Challenge

- Calibrating this linear function requires knowing the points of maximum and minimum phenological stages of crop due to water stress. This information is not easily obtainable, and uncertainties in this knowledge can introduce errors into the estimation.

Solution

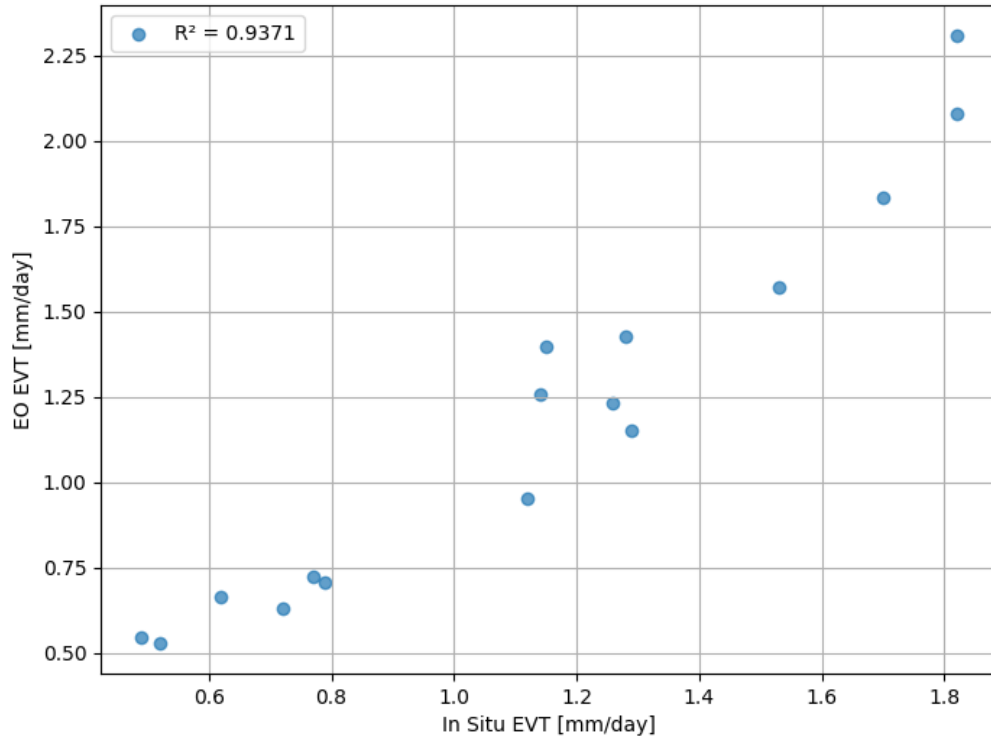
- To minimize sources of uncertainty and enhance the reliability of the subsequent comparisons and analyses with EO data from PRISMA, Sentinel-2, and Landsat sensors, the K_s value was directly taken from in-situ measurements. This method was chosen to eliminate any potential inaccuracies that could arise from using remote thermal measurements, which can be affected by various atmospheric and sensor-specific factors or introduced by the methodology used to derive the K_s .

16/06/23 Prisma VNIR & Landsat Thermal data

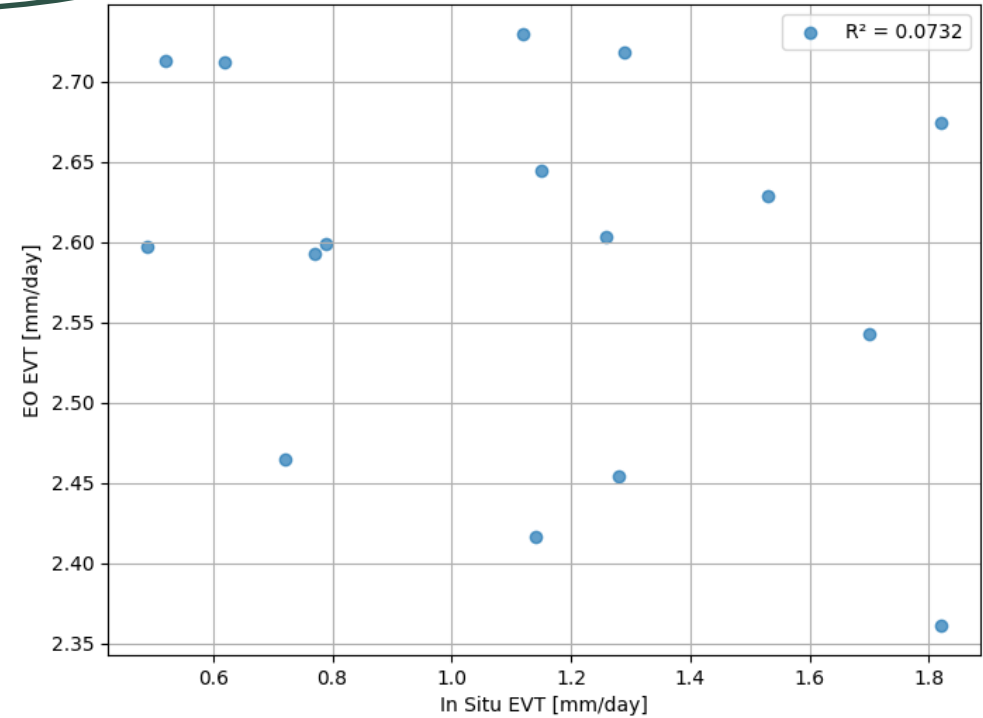


05/01/24 Prisma VNIR & Landsat Thermal data

EO EVT (using Ks from in situ) vs In Situ EVT



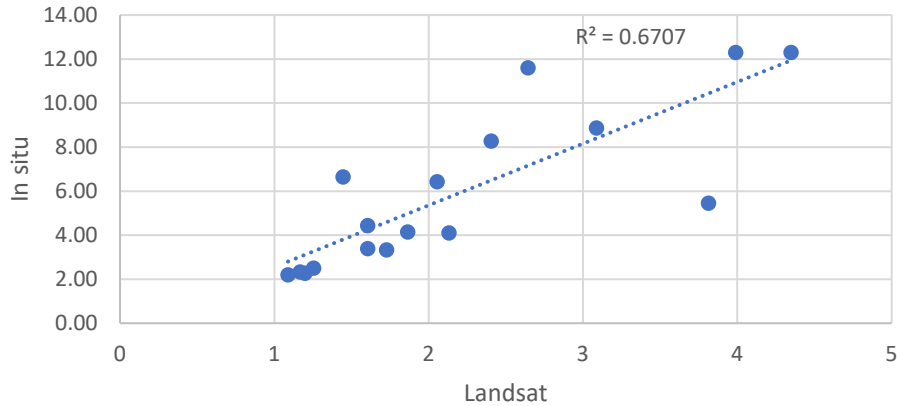
EO EVT vs In Situ EVT



Per Pivot comparison Season 1 (May-September 2023)

Landsat

Eta with Ks from in situ (mm/day)

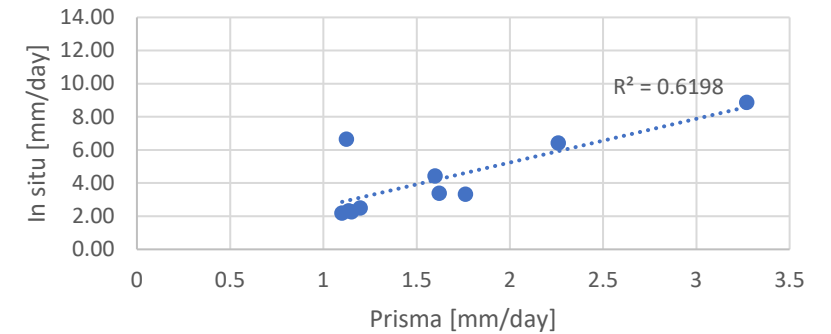


PN1

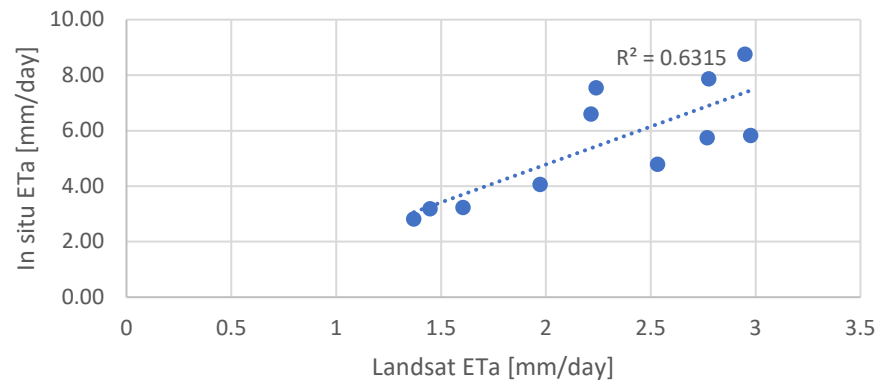


Prisma

ETa calculated with Ks from in situ (mm/day)



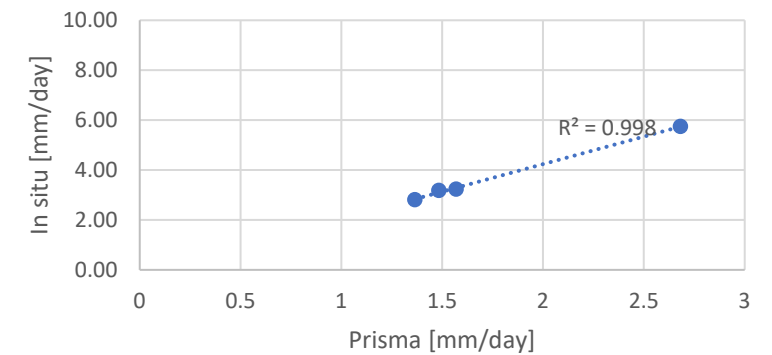
Eta calculated with Ks from in situ (mm/day)



PN2



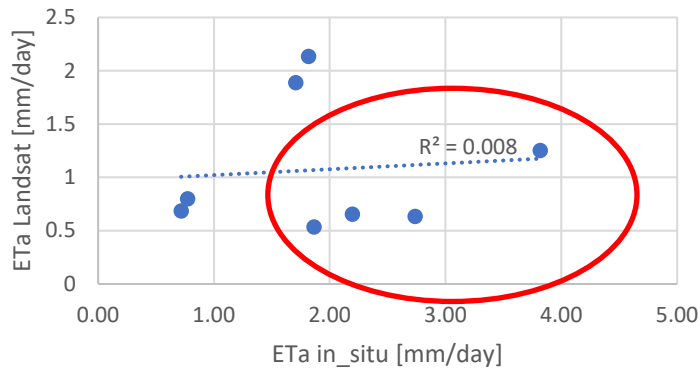
ETa calculated with Ks from in situ (mm/day)



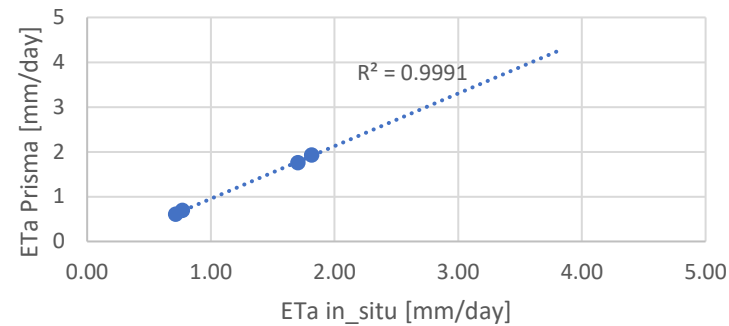
Per Pivot comparison Season 2 (December-April 2024)

Challenge : Very few field measurements ! Many missing dates ! High in situ EVT values paradox ??

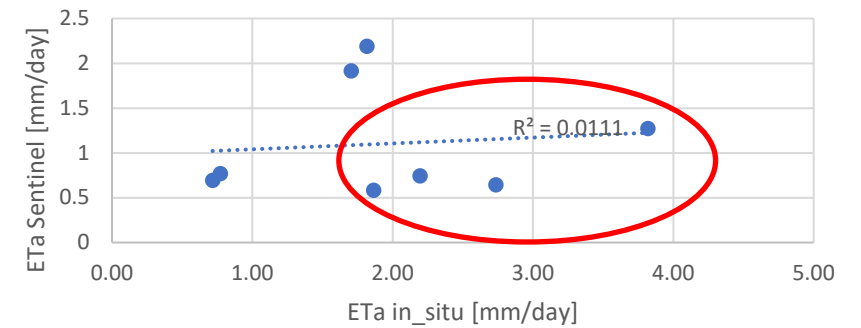
Eta_intermediate Landsat



Eta_Intermediate Prisma



Eta_Intermediate Sentinel

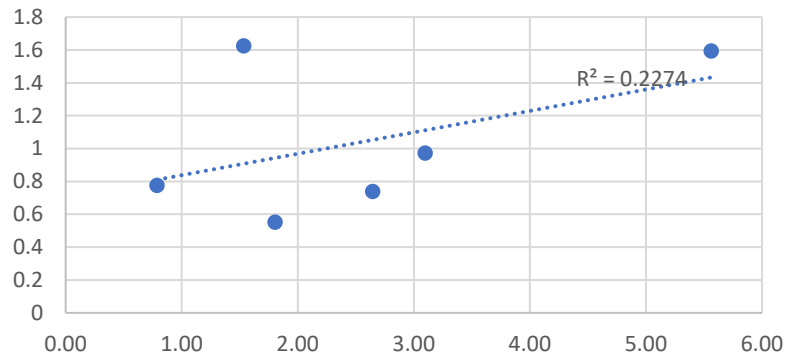


06/01/24 & 03/04/24 field measurements for PN2.

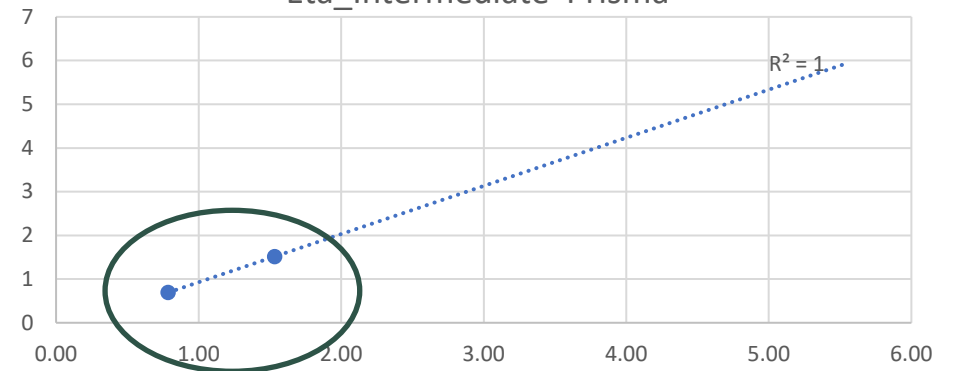
In total 4-8 data points to compare, where 03/04/24 in situ ones really high

In total 2-6 data points to compare, where 03/04/24 in situ ones really high for PN3

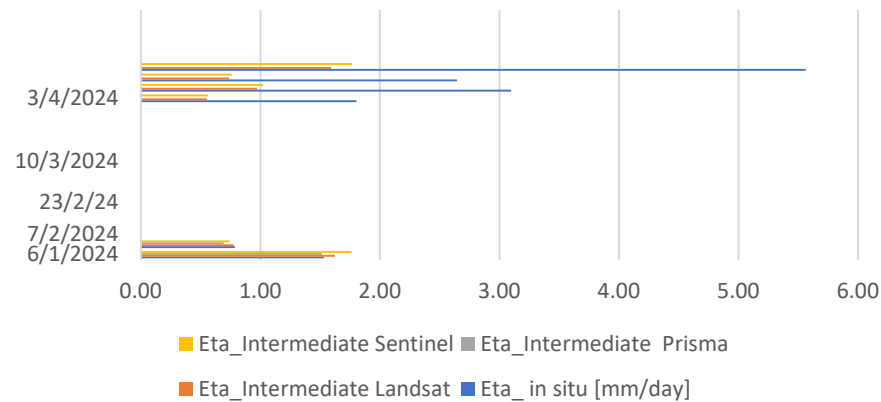
Eta_Intermediate Landsat



Eta_Intermediate Prisma

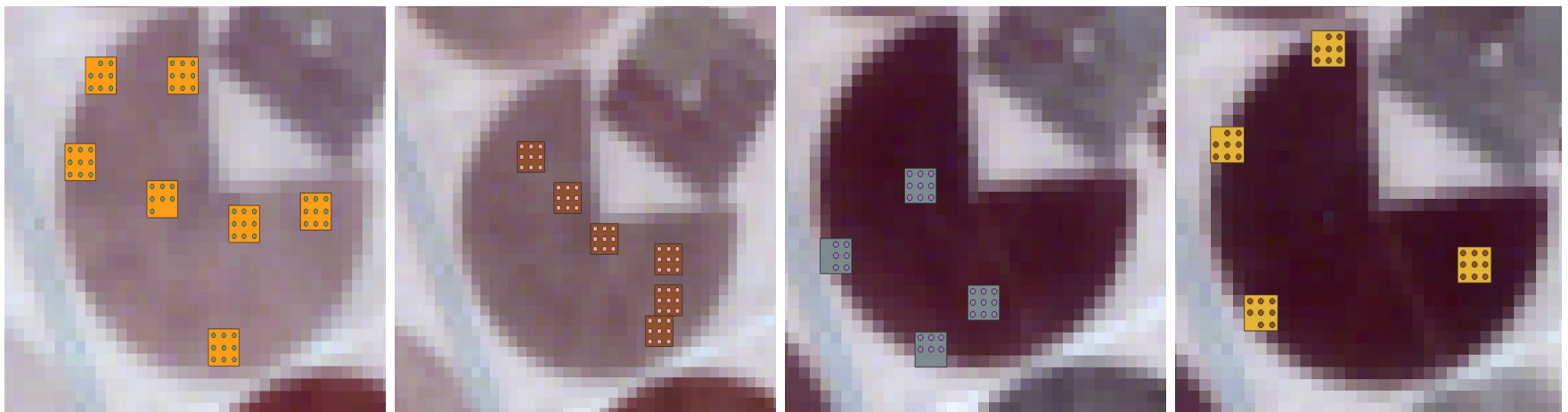


PN3



ML Approaches

Data collection and dataset building



| Date | Sample sites [n°] | Sampled pixels [n°] |
|-------|-------------------|---------------------|
| 06/06 | 7 | 87 |
| 16/06 | 21 | 117 |
| 14/07 | 13 | 182 |
| 22/07 | 13 | 113 |

Location data

| Date | Pivots | Sample | Lat | Long |
|-------|--------|--------|---------|---------|
| 06_06 | PN1 | F2S1 | 30.4539 | 31.9965 |
| 06_06 | PN1 | F2S1 | 30.4539 | 31.9965 |
| 06_06 | PN1 | F2S1 | 30.4539 | 31.9965 |
| 06_06 | PN1 | F2S1 | 30.4539 | 31.9965 |
| 06_06 | PN1 | F2S1 | 30.4539 | 31.9965 |
| 06_06 | PN1 | F2S1 | 30.4539 | 31.9965 |
| 06_06 | PN1 | F2S1 | 30.4539 | 31.9965 |

Prisma – VNIR - SWIR

| 06_06_NI R_1 | 06_06_NI R_2 | 06_06_NI R_3 | 06_06_NI R_4 | 06_06_NI R_5 | 06_06_NI R_6 | 06_06_NI R_7 |
|-----------------|-----------------|-----------------|-----------------|-----------------|-----------------|-----------------|
| 3563 | 3291 | 4122 | 4341 | 4831 | 5279 | 5627 |
| 2995 | 2829 | 3089 | 3246 | 4412 | 4569 | 4760 |
| 4246 | 4089 | 4958 | 4661 | 6066 | 6834 | 6703 |
| 3271 | 3235 | 3528 | 3465 | 4713 | 5061 | 5056 |
| 3804 | 3149 | 3439 | 3378 | 4643 | 4659 | 4871 |
| 3187 | 2972 | 3085 | 3276 | 4392 | 4475 | 4596 |
| 3169 | 3541 | 4262 | 4307 | 5018 | 5353 | 5634 |

Landsat

| Landsat_ B1 | Landsat_ B2 | Landsat_ B3 |
|-------------|-------------|-------------|
| 10549 | 11406 | 14276 |
| 10329 | 11097 | 13815 |
| 10775 | 11622 | 14616 |
| 10356 | 11160 | 13671 |
| 10525 | 11361 | 14221 |
| 10464 | 11247 | 14055 |
| 10521 | 11403 | 14358 |
| 10200 | 11007 | 13763 |

In-situ

| TDR | ETO | Kc | Ks | ETa |
|------|-----|-----|------|------|
| 11.5 | 8.1 | 0.7 | 0.49 | 2.79 |
| 11.5 | 8.1 | 0.7 | 0.49 | 2.79 |
| 11.5 | 8.1 | 0.7 | 0.49 | 2.79 |
| 11.5 | 8.1 | 0.7 | 0.49 | 2.79 |
| 11.5 | 8.1 | 0.7 | 0.49 | 2.79 |
| 11.5 | 8.1 | 0.7 | 0.49 | 2.79 |
| 11.5 | 8.1 | 0.7 | 0.49 | 2.79 |

- 4 different dates
- 54 sample sites
- pixel sampled for both Landsat8 and PRISMA images



ML Approaches

Algorithms and preliminary results



2 algorithms used:

- Light Gradient Boosting Model (LGBM) regressor;
- Random Forest (RF) regressor;
- R^2 used for prediction accuracy estimation;

| Algorithms | Accuracy R-squared | | |
|------------|--------------------|------|------|
| | Kc | Ks | ETa |
| LGBM | 0.88 | 0.15 | 0.73 |
| RF | 0,88 | 0,05 | 0.54 |

| Importance x predicted parameter | | | | | | | | |
|----------------------------------|-------------|-------------|-------------|-------------|---------|-------------|---------|-------------|
| | LGBM | | | | RF | | | |
| | Kc | Ks | ET0 | ETa | Kc | Ks | ET0 | ETa |
| Band/Hyperspectral index | Landsat_B10 | ndmi | ndmi | Landsat_B10 | VNIR_24 | VNIR_4 | VNIR_24 | LST |
| | VNIR_1 | SWIR_41 | Landsat_B10 | VNIR_40 | VNIR_23 | VNIR_3 | VNIR_21 | Landsat_B10 |
| | ndmi | VNIR_40 | SWIR_49 | SWIR_102 | VNIR_25 | ndmi | VNIR_23 | ndmi |
| | VNIR_40 | SWIR_97 | VNIR_39 | ndmi | VNIR_22 | SWIR_86 | VNIR_25 | SWIR_49 |
| | SWIR_99 | SWIR_40 | VNIR_1 | wi | SWIR_22 | Landsat_B10 | VNIR_27 | SWIR_50 |
| | VNIR_42 | SWIR_89 | SWIR_93 | SWIR_42 | SWIR_41 | SWIR_42 | VNIR_28 | srwi |
| | SWIR_3 | Landsat_B10 | srwi | SWIR_95 | VNIR_19 | SWIR_136 | VNIR_29 | VNIR_1 |
| | CSWI | SWIR_35 | VNIR_40 | SWIR_101 | SWIR_49 | srwi | ndvi | VNIR_2 |
| | SWIR_49 | SWIR_98 | VNIR_9 | CSWI | ndmi | LST | LST | VNIR_3 |
| | srwi | SWIR_91 | VNIR_6 | SWIR_97 | VNIR_20 | VNIR_2 | ndmi | VNIR_4 |



Search

Register Sign in

EO Africa





Data Maps Dashboards

Home About English

Filter 2 Resources found

Order by


EO Africa
EO Africa dashboard
GIS Manager [View](#)


Alldatesvsinsitu.xlsx
No abstract provided
Nick Pappas [View](#)

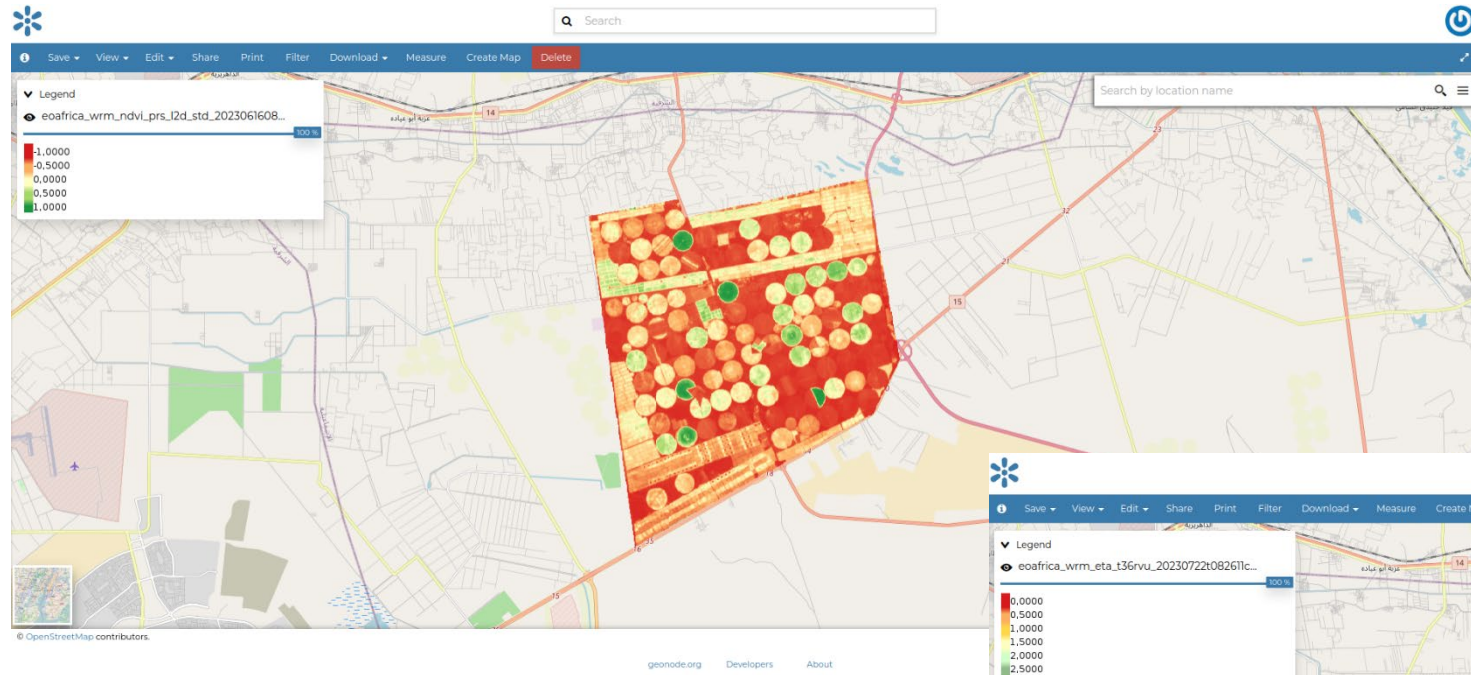
Login/Landing Page

The EO Africa Platform

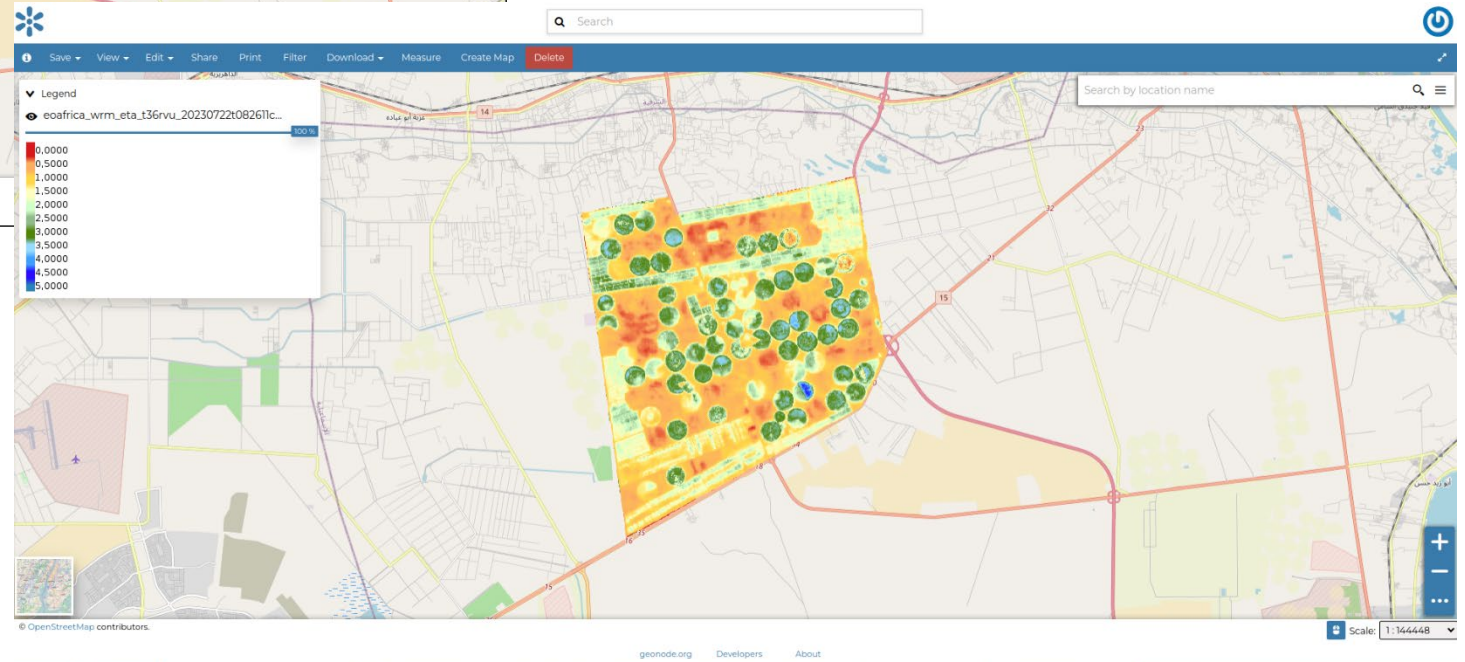


Time series selection





Product selection





- The ECOSTRESS challenge
- Few data points in each field visit. One field visit at each visit gives 4-7 field measurements to compare.
- Timing Discrepancy in Data Collection: The limited number of monitoring dates, influenced by the specific pivot being considered, highlights a critical challenge in synchronizing Earth Observation (EO) data acquisitions with in-situ data collection.
- Phenological Stage-Dependent Monitoring Needs: Crop growth stages exhibit varying monitoring requirements. Early stages may need less frequent monitoring, whereas advanced stages, particularly during peak irrigation demands, require more frequent satellite overpasses to capture critical data.
- In-Situ Data Accuracy Challenges: Low coefficients of determination between EO and in-situ data can stem from inaccuracies in traditional in-situ data collection methods.



- Discrepancy in Soil Moisture Measurements: There is a notable mismatch between soil moisture levels obtained via EO thermal data (CWSI) and in-situ measurements (TDR probe). This discrepancy may be attributed to factors like soil water retention, solar radiation, or wind speed, which impact the relationship between soil moisture and vegetation health.
- Impact of Spatial Resolution on Leaf Temperature Assessment: Leaf temperature, derived from satellite data, is effective for assessing crop water status. However, the 30-meter spatial resolution may introduce errors, particularly at the endpoints of pivots, where the influence of bare soil can distort land surface temperature values, complicating the identification of “hot” and “cold” spots in vegetation.



- Hyperspectral sensors give promising results and provide an alternative in terms of wavelength choices , giving the opportunity to adjust/work with different bands and indexes
- Understand the Season 1 and Season 3 similarities and find a common perspective for each season to use as calibration
- Leverage the good R^2 ML approach gives so far .
 - Either use the ML results as calibration parameters to the SARE model approach results
 - Either use some algorithms from the LGBM model and customize to the developed algorithm
 - Tries to be independent from Ks index as this introduces many risks in terms of prediction no matter the method used regarding EO data



Thank you !

